2016 International Symposium on Nonlinear Theory and Its Applications,
NOLTA2016, Yugawara, Japan, November 27th-30th, 2016

Stability Analysis of Phase-Inversion Waves in Coupled Piecewise-Constant Oscillators As a Ladder

Ryohei Hirota† and Tadashi Tsubone‡

†Nagaoka University of Technology
1603-1, Kamitomioka, Nagaoka, Niigata, 940-2188, Japan
Email: s133165@stn.nagaokaut.ac.jp
‡Nagaoka University of Technology
Email: tsubone@vos.nagaokaut.ac.jp

Abstract—In this study, we consider phase-inversion waves in coupled piecewise-constant oscillators as a ladder. A nonlinear phenomenon called phase-inversion wave is a kind of wave propagation phenomena, and the phase states of the waves are propagated to next oscillator in succession. In this paper, we analyzed the stability of the phase-inversion waves using the largest Lyapunov exponent. As a result, we found out that phase-inversion waves is unstable and chaos, because the largest Lyapunov exponent is positive value.

1. Introduction

There are many reports for analysis of synchronization phenomena of coupled oscillators [1–5]. Suzuki and Tsubone have confirmed that piecewise-constant oscillators coupled by hysteresis elements exhibit co-existence of in-phase and anti-phase synchronization [1]. They also analyzed the stability of the system by Lyapunov exponents. Yamauchi, Nishio, and Ushida have discovered wave propagation phenomena called phase-inversion waves of coupled van der Pol oscillators [2, 3]. The phase-inversion waves are wave propagation phenomena, and the phase states of the waves are propagated to next oscillator in succession. It is very important to analyze the phenomena, because it is similar to propagation phenomena of electrical information in an axial fiber of nervous systems. However, if nonlinearity of van der Pol oscillators are strong, the analysis often becomes hard. The simulation requires high calculation cost. When we carry out Lyapunov analysis for high dimensional system, sometimes very long time is needed. Therefore, confirmation of phase-inversion waves in rigorous sense and detailed stability analysis of the systems which generate the phase-inversion waves have not been discussed. Accordingly, we consider piecewise-constant oscillators. The oscillators are simple systems and the analysis is relatively easy. The systems have piecewise-constant vector fields, and the solutions are piecewise-linear. Hence, we have only to focus on the borders of switching of the vector fields, we can determine the rigorous solutions [1]. Using the calculation method [1], we can derive the rigorous solution with low calculation cost. In this paper, we show phase-inversion waves of coupled three piecewise-constant oscillators. We also analyze the stability of the phase-inversion waves in our system by the largest Lyapunov exponent. As a result, we found out that phase-inversion waves is chaos, because the largest Lyapunov exponent is positive value. It can be obtained rigorously from computer-aided analyzing procedure by using rigorous solutions.

2. Circuit model

2.1. A Piecewise-Constant Oscillator

Figure 1 shows a circuit model of a piecewise-constant oscillator.

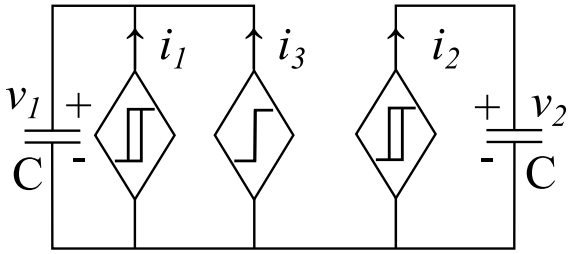

Fig. 1 Cicuit model of a piecewise-constant oscillator.

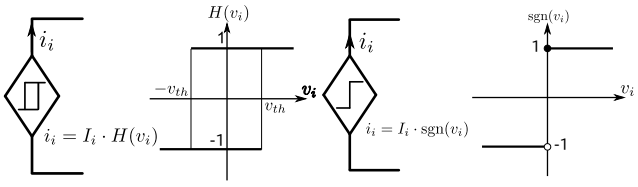

(a)VCCS with hysteresis characteristic.

(b)VCCS with Signum-like function.

Fig. 2 Symbols and nonlinear characteristics of VCCSs.

The circuit equations of the system are described as follows.

$$\begin{cases} C\dfrac{\mathrm{d}v_1}{\mathrm{d}t} = I_1 \cdot H(v_1) + I_3 \cdot \mathrm{sgn}(v_2), \\ C\dfrac{\mathrm{d}v_2}{\mathrm{d}t} = I_2 \cdot H(v_1), \end{cases} \tag{1}$$

where I_1, I_2 and I_3 are absolute values of output currents of hysteresis or sgn Voltage Controlled Current Sources(VCCSs). We consider the following conditions.

$$I_2 = -I_3, \quad I_1 \cdot I_2 < 0. \tag{2}$$

The conditions (2) guarantees non-constrained behaviors. $H(v_{in})$ and $\mathrm{sgn}(v_{in})$ are hysteresis and signum characteristic respectively, as shown in Fig. 2. We use following dimensionless variables and parameters

$$\tau = \frac{I_2}{C \cdot v_{th}} t, \; x = \frac{v_1}{v_{th}}, \; y = \frac{v_2}{v_{th}}, \; \alpha = -\frac{I_1}{I_2}. \tag{3}$$

Then, we can rewrite the circuit Eq. (1) as following dynamics,

$$\begin{cases} \dot{x} = -\alpha h(x) - \mathrm{sgn}(y) \\ \dot{y} = h(x), \end{cases} \tag{4}$$

where "$\cdot$" denote differentiation by normalized time τ, $h(X)$ shows normalized hysteresis. If X reaches 1, the output switches from -1 to 1, and if X reaches -1, output switches from 1 to -1. The system has only one parameter α. In order to oscillate, we consider the following conditions [1].

$$0 < \alpha < 1. \tag{5}$$

Figure 3 shows a rigorous solution and the corresponding laboratory measurement.

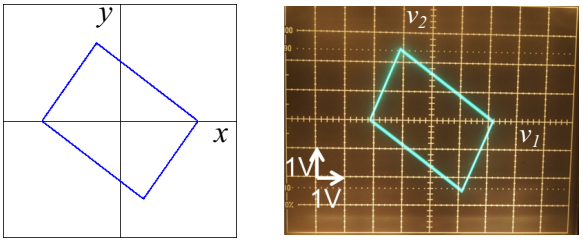

(a)Rigorous solution. (b)Laboratory measurement.

Fig. 3 Rigorous solution and laboratory measurement of a piecewise-constant oscillator.

2.2. Piecewise Constant Oscillators Coupled by hysteresis element as a Ladder

We consider piecewise-constant oscillators coupled by hysteresis elements as a ladder. Figure 4 shows circuit model of the coupled piecewise-constant oscillators. This system has following dynamics.

[First oscillator] $(m = 1)$

$$\begin{cases} \dot{x_1} = -\alpha h(x_1) - \mathrm{sgn}(y_1) - \gamma h(x_1 - x_2) \\ \dot{y_1} = h(x_1), \end{cases} \tag{6}$$

[Middle oscillator] $(2 \le m \le N-1)$

$$\begin{cases} \dot{x_m} = -\alpha h(x_m) - \mathrm{sgn}(y_m) \\ \qquad -\gamma h(x_m - x_{m+1}) + \gamma h(x_{m-1} - x_m) \\ \dot{y_m} = h(x_m), \end{cases} \tag{7}$$

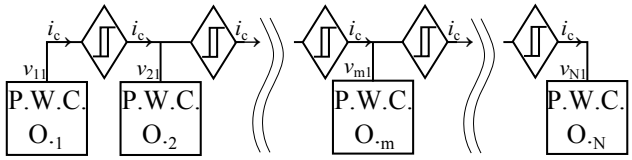

Fig. 4 Circuit model of coupled piecewise-constant oscillators by hysteresis elements.

[Last oscillator] $(m = N)$

$$\begin{cases} \dot{x_N} = -\alpha h(x_N) - \mathrm{sgn}(y_N) + \gamma h(x_{N-1} - x_N) \\ \dot{y_N} = h(x_N). \end{cases} \tag{8}$$

The system has two parameters, α and γ. N is number of oscillators, and γ is a coupling parameter. In this paper, we discuss the case of $N = 3$. In our previous study, we observed phase-inversion waves in this system [5]. Figure 5 shows a rigorous solution and the corresponding laboratory measure ment.

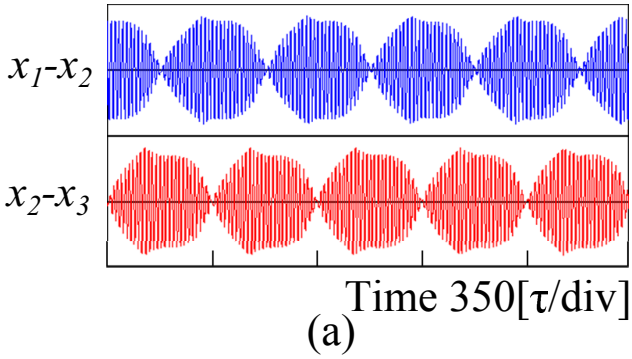

Rigorous solution.

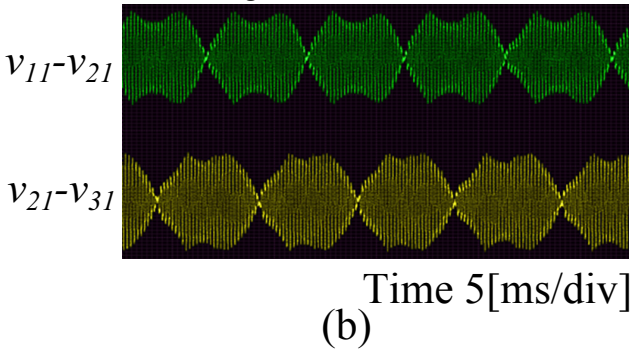

Laboratory measurement.

Fig. 5 Phase-inversion waves in rigorous solution and laboratory measurement

Figure 5 represents the difference between output of adjacent oscillators. Small waves are in-phase, and large waves are anti-phase synchronization. We can observe changing phase state, namely phase-inversion waves.

3. Calculation of rigorous solution and Lyapunov exponent

In piecewise-constant system, we can obtain the rigorous solution directly by noting borders of vector fields [1]. The borders are points that h or sgn switches. For easy to explain, we introduce the algorithm for solution be given a piecewise-constant oscillator in this section. A trajectory starts initial point $\boldsymbol{x_0} = (x_0, y_0)$, and goes straight forward to border$E$ in accordance with vector field $a(i)$ in Table 1. A time to reach the border τ is obtained by

$$\tau_x = \frac{E_x(i) - x}{\dot{x}}, \ \tau_y = \frac{E_y(i) - y}{\dot{y}}, \tag{9}$$

where τ is positive and minimum value. We calculate $\boldsymbol{x_{k+1}}$ using τ and $\boldsymbol{x_k}$.

$$\boldsymbol{x_{k+1}} = \boldsymbol{x_k} + \boldsymbol{a}(i_k) \cdot \tau. \tag{10}$$

In the same manner, we can also obtain $\boldsymbol{x_2}$, $\boldsymbol{x_3}$... and derivate rigorous solution, like Fig. 6.

Table 1: Local vector fields and borders for i.

i	$h(x)$	sgn(y)	$\boldsymbol{a}(i)$	$E_x(i)$	$E_y(i)$
0	1	1	${}^t(-\alpha - 1, 1)$	-1	0
1	1	-1	${}^t(-\alpha + 1, 1)$	-1	0
2	-1	1	${}^t(\alpha - 1, -1)$	1	0
3	-1	-1	${}^t(\alpha + 1, -1)$	1	0

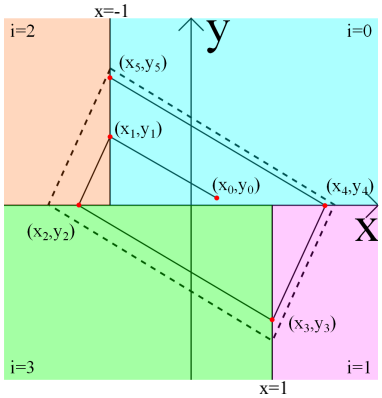

Fig. 6 Trajectory of a piecewise-constant oscillator.

We can calculate Lyapunov exponent using this algorithm for the rigorous solution. Because Eq. (10) is linear mapping equation, deforming right side of Eq. (10) and differentiating by $\boldsymbol{x_k}$, we can obtain Jacobian matrix J_k.

$$\begin{aligned} \boldsymbol{x_{k+1}} &= \boldsymbol{x_k} + \boldsymbol{a}(i_k) \cdot \tau. \\ &= A \cdot \boldsymbol{x_k}, \qquad (11) \\ J_k &= \frac{\partial \boldsymbol{x_{k+1}}}{\partial \boldsymbol{x_k}} \qquad (12) \end{aligned}$$

We calculate Lyapunov exponents by applying J_k to Shimada algorithm. [6] In this report, we calculated the largest Lyapunov exponent λ_1. This value is given by

$$\begin{aligned} \lambda_1 &= \lim_{L \to 10^8} \frac{1}{L} \sum_{k=1}^{L} \ln \| J_k e_1^k \|, \\ e_1^{k+1} &= \frac{J_k e_1^k}{\| J_k e_1^k \|}, \end{aligned} \tag{13}$$

where e_k is orthonormal base, and L is iteration number. We set L to 10^8 as large enough.

4. Lyapunov analysis

Figure 7 is a two-parameter bifurcation diagram. The vertical axis is α and the horizontal axis is γ. In the figure, black and gray regions show $\lambda_1 > 0$. White regions show $\lambda_1 = 0$. Reds show $\lambda_1 < 0$. We defined that $|\lambda_1| < 10^{-7}$ is $\lambda_1 = 0$ [7].

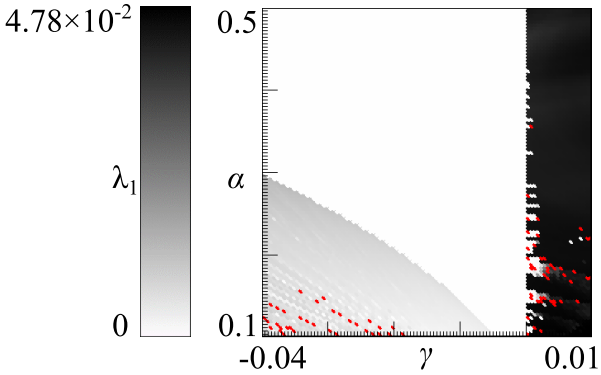

Fig. 7 Two-parameter bifurcation diagram in $\gamma - \alpha$ plane.

In gray regions, we can observe phase-inversion waves. On the other hand, we can observe in-phase or almost in-phase synchronization phenomena in white regions.

Next, we compared waveforms in gray and white regions. Figure 8 and 9 show output differences in $(\gamma, \alpha) = (-0.03, 0.2)$ and $(\gamma, \alpha) = (-0.03, 0.3)$.

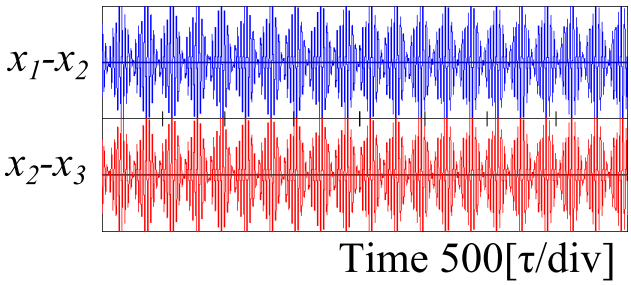

Fig. 8 The difference between output of adjacent oscillators in $\lambda_1 > 0$(Gray region).

In Fig. 8, phase-inversion wave happens and the largest Lyapunov exponent is $\lambda_1 = 7.3421 \times 10^{-3} > 0$. On the

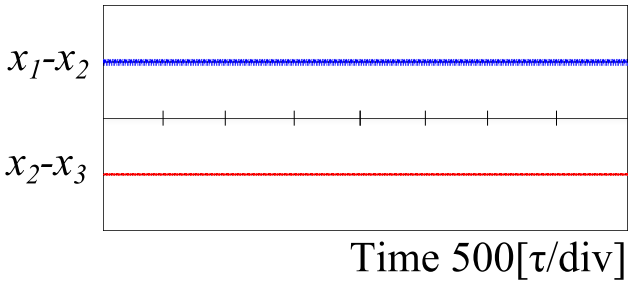

Fig. 9 The difference between output of adjacent oscillators in $\lambda_1 \simeq 0$(White region).

other, in-phase synchronization happens and the largest Lyapunov exponent is $\lambda_1 = 1.2437 \times 10^{-9} \simeq 0$ in Fig. 9. Figure 9 looks like periodic motion. However, when we confirm waveforms of longtime, we found that this is non-periodic motion. In Fig. 10, we can see that waveforms

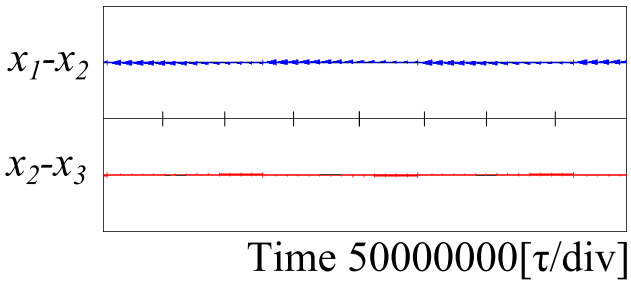

Fig. 10 Longtime waveforms of Fig. 9.

change subtly.

We show output differences in other parameters. Figure

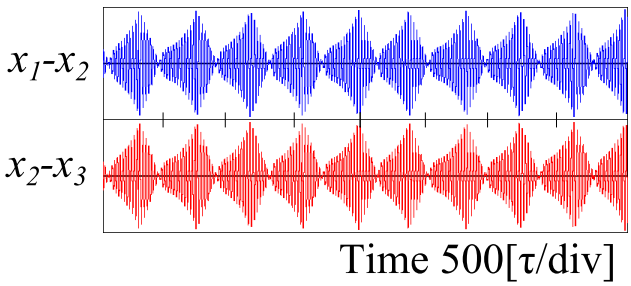

Fig. 11 The difference between output of adjacent oscillators in the other parameters (1).

11 and 12 show output differences in $(\gamma, \alpha) = (-0.02, 0.2)$ and $(\gamma, \alpha) = (-0.01, 0.1)$. The largest Lyapunov exponents are both positive value. Thus, we can observe another type phase-inversion waves, but we can not divide these phenomena with the largest exponent.

5. Conclusion

In this paper, we considered phase-inversion waves of three piecewise-constant oscillators coupled by hysteresis

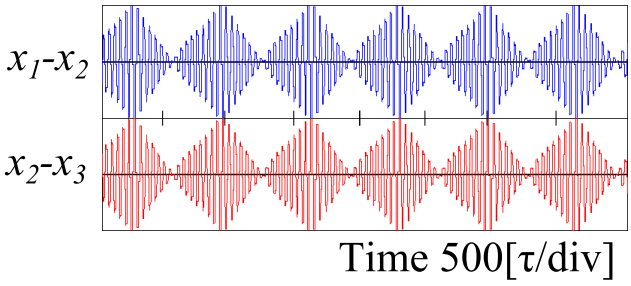

Fig. 12 The difference between output of adjacent oscillators in the other parameters (2).

elements as a ladder. We carried out stability of phase-inversion waves with the largest Lyapunov exponent. As a result, we found that phase-inversion waves are unstable and chaos because the largest Lyapunov exponent is positive value. Our future tasks are calculating the 2nd and 3rd largest Lyapunov exponents and analyzing in more detail by using these numbers.

References

[1] K. Suzuki and T. Tsubone, “In-Phase and Anti-Phase Synchronization Phenomena in Coupled Systems of Piecewise Constant Oscillators”, IEICE Trans. Fundamentals, Vol. E98-A No. 1, pp. 340-353, (2015)

[2] M. Yamauchi, Y. Nishio, and A. Ushida, “Phase-Waves in a Ladder of Oscillators”, IEICE Trans. Fundamentals, Vol. E86-A, No. 4, pp. 891-899, (2003)

[3] M. Yamauchi, Y. Nishio, and A. Ushida, “Analysis of Phase-Inversion Waves in Coupled oscillators Synchronizing at In-and-Anti-Phase”, IEICE Trans. Fundamentals, Vol. E86-A, No. 7, pp. 1799-1806, (2003)

[4] D. P. Rosin, D. Rontani, and D. J. Gauthier, “Synchronization of Boolean phase oscillators”, Phys. Rev. E 89, 042907, (2014)

[5] R. Hirota and T. Tsubone, “Analysis of Phase-Inversion Waves in Coupled Piecewise Constant Oscillators as a Ladder”, Proc. of NOLTA2015, pp.101-104, (2015)

[6] I. Shimada, and T. Nagashima, “A Numerical Approach to Ergodic Problem of Dissipative Dynamical Systems”, Prog. Theor. Phys., Vol. 61, No. 6, pp. 1605-1616, (1979)

[7] S. Hidaka, N, Inaba, K, Kamiyama, M, Sekikawa, and T, Endo, “Bifurcation structure of an invariant three-torus and its computational sensitivity generated in s three-coupled delayed logistic map”, NOLTA, vol.6 No. 3, pp. 433-442, (2015)